

SUPPLEMENTARY INFORMATION

Structure, luminescence and magnetic properties of an erbium(III) β -diketonate homodinuclear complex

P. Martín-Ramos,^{a,b} L.C.J. Pereira,^{*c} J.T. Coutinho,^c F. Koprowiak,^d H. Bolvin,^d V. Lavín,^e I.R. Martín,^e J. Martín-Gil^f and M. Ramos-Silva^{*b}

^a EPSH, Universidad de Zaragoza, Carretera de Cuarte s/n, 22071, Huesca, Spain.

^b CFisUC, Department of Physics, Universidade de Coimbra, Rua Larga, P-3004-516 Coimbra, Portugal.

^c C2TN, DECNentro de Ciências e Tecnologias Nucleares, Instituto Superior Técnico, Universidade de Lisboa, 2695-066 Bobadela LRS, Portugal.

^d Laboratoire de Chimie et Physique Quantiques, Université Toulouse III, 118 route de Narbonne, 31062 Toulouse, France.

^e Departamento de Física and MALTA Consolider Team, Universidad de La Laguna, E-38206 San Cristóbal de La Laguna, Santa Cruz de Tenerife, Spain.

^f Advanced Materials Laboratory, ETSIIAA, Universidad de Valladolid, Avenida de Madrid 44, 34004, Palencia, Spain.

* Corresponding authors: manuela@pollux.fis.uc.pt, lpereira@ctn.ist.utl.pt

Contents:

1. Structural data
2. X-ray powder diffraction
3. Thermal analysis
4. Vibrational characterization
5. Optical characterization
6. Magnetic measurements
7. Theoretical Calculations

1. Structural data

Table S1. Selected distances and angles (Å,°)

Bond	Distance	Bonds	Angle
Er1-O1	2.305(2)	O2-Er1-O1	73.42(7)
Er1-O2	2.292(2)	O3-Er1-O4	74.70(7)
Er1-O3	2.283(2)	O5-Er1-O6	74.62(7)
Er1-O4	2.286(2)	O3-Er1-O1	118.01(6)
Er1-O5	2.290(3)	O4-Er1-O1	79.09(6)
Er1-O6	2.300(2)	O5-Er1-O1	78.44(7)
Er1-N1	2.580(2)	O6-Er1-O1	149.29(8)
Er1-N2	2.583(3)	O1-Er1-N1	135.55(6)
Er-O avg.	2.293	O2-Er1-N2	70.84(7)
Er-N avg.	2.582	N1-Er1-N2	62.63(6)

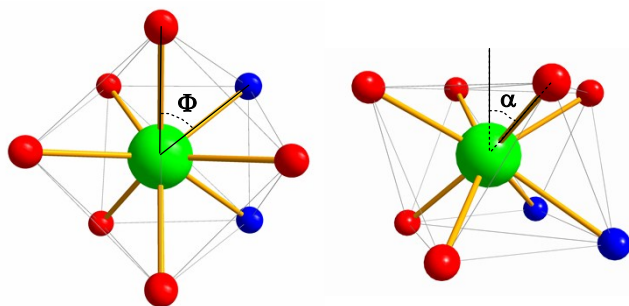


Figure S1. Definition of Φ and α in the square-antiprismatic geometry, taking the first coordination sphere of Er1 as an example.

2. X-ray powder diffraction

The experimental diffractograms in Figure S2 show a background higher for low theta angles as expected from the diffuse scattering of X-rays by glass and air, a common characteristic when using rotating capillaries in a Debye-Scherrer geometry. Powder diffraction shows that all the material synthesized contains the same structure as the small single crystals used for single-crystal X-ray diffraction.

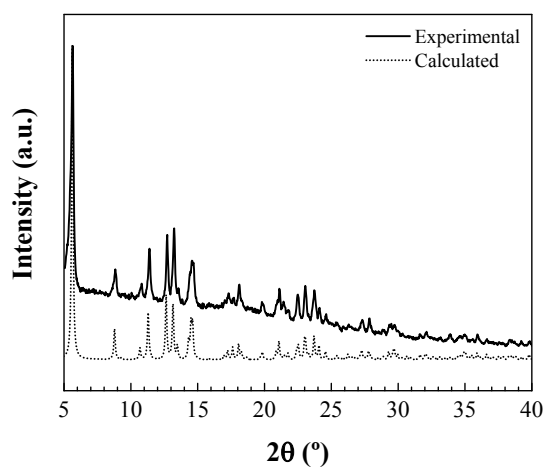


Figure S2. Experimental (*solid line*) vs. simulated (*dotted line*) X-ray powder diffraction patterns for the complex.

3. Thermal analysis

The DSC curve of $[\text{Er}_2(\text{nd})_6(\mu\text{-bpm})]$ complex is depicted in Figure S3.

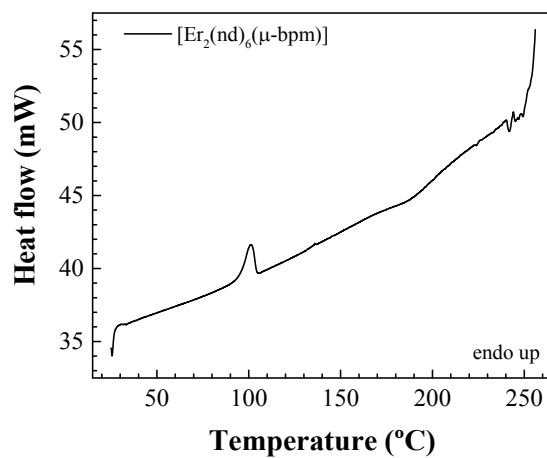


Figure S3. DSC curve of $[\text{Er}_2(\text{nd})_6(\mu\text{-bpm})]$ complex.

4. Vibrational characterization

The ATR-FTIR spectrum of $[\text{Er}_2(\text{nd})_6(\text{bpm})]$ is shown in Figure S4.

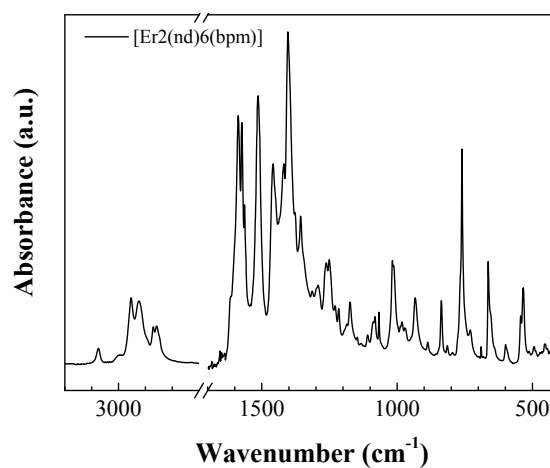


Figure S4. ATR-FTIR spectrum of $[\text{Er}_2(\text{nd})_6(\mu\text{-bpm})]$.

5. Optical characterization

Photoluminescence in the visible range

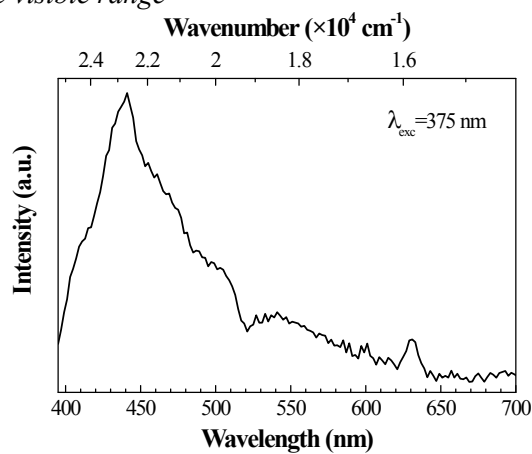


Figure S5. Photoluminescence spectrum in the visible region for $[\text{Er}_2(\text{nd})_6(\mu\text{-bpm})]$ upon excitation at 375 nm.

NIR photoluminescence spectrum

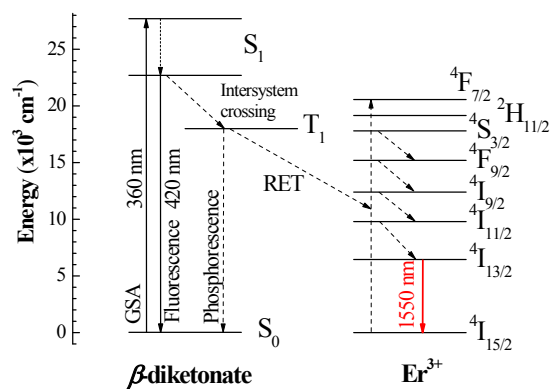


Figure S6. Scheme of the energy transfer mechanisms and emission processes.

6. Magnetic measurements

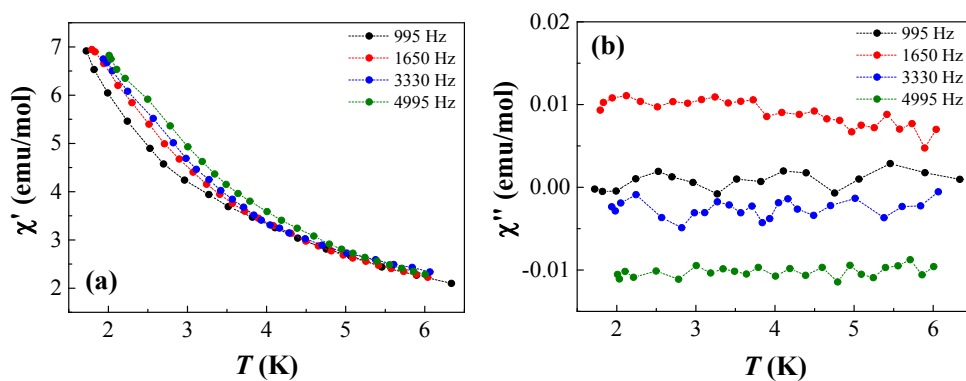


Figure S7. (a) In-phase and (b) out-of-phase components of the AC susceptibility at different frequencies in the 1.7–6.5 K temperature range for the $[\text{Er}_2(\text{nd})_6(\mu\text{-bpm})]$ complex. $H_{\text{AC}}=5$ Oe; $H_{\text{DC}}=0$ Oe.

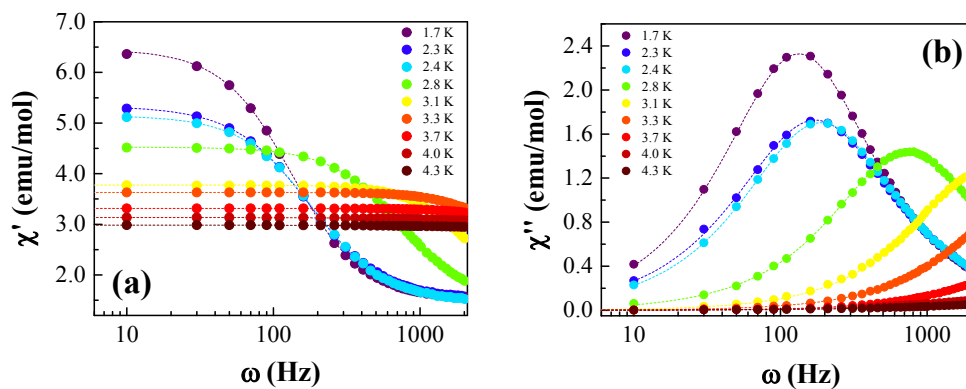


Figure S8. (a) In-phase, and (b) out-of-phase components of the AC susceptibility at different frequencies in the 1.7–4.3 K temperature range for the $[\text{Er}_2(\text{nd})_6(\mu\text{-bpm})]$ complex. Debye fittings are shown as dashed lines. $H_{\text{AC}}=5$ Oe; $H_{\text{DC}}=1000$ Oe.

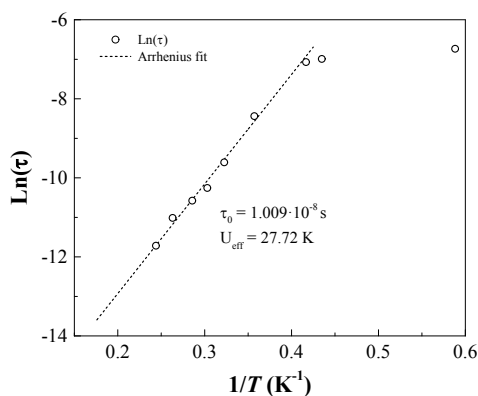


Figure S9. Arrhenius Law fitting for $[\text{Er}_2(\text{nd})_6(\mu\text{-bpm})]$ complex. $H_{\text{AC}}=5$ Oe, $H_{\text{DC}}=1000$ Oe.

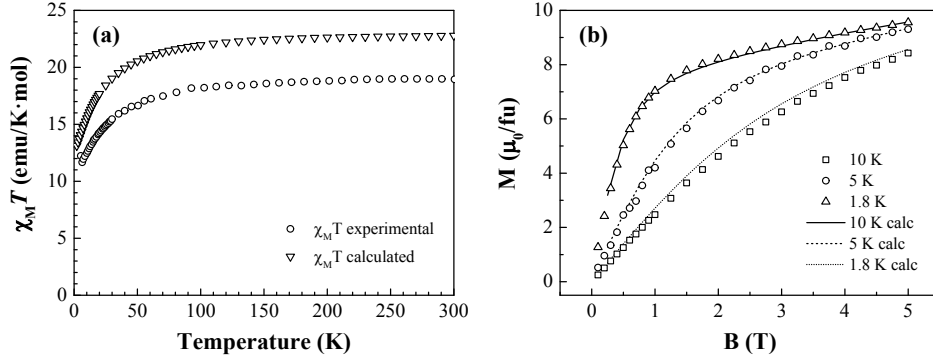


Figure S10. Experimental and calculated values for: (a) temperature dependence of the χT product; (b) magnetization vs. applied field.

7. Theoretical calculations

A local modification of MOLCAS was used to generate natural spin orbitals (NSOs) from SO-CASSCF calculations. Within the frame of the principal magnetic axes of the doublet ground state X , Y and Z , to generate the NSOs ϕ_p^u in direction $u = X, Y, Z$, one considers linear combinations of the ground state doublet components $|\Psi_0^u\rangle$ diagonalizing the magnetic moment operator \hat{M}_U and the NSOs ϕ_i^u are the eigen-functions of the one-particle spin-magnetization density matrices. It results that when the external magnetic field is applied along direction u , the spin density is

$$\rho^u(r) = \sum_{i=1}^7 n_i \phi_i(r)^2 \quad \text{where } \phi_i \text{ is the NSO}_i \text{ with occupation } n_i. \text{ The spin magnetization in this}$$

$$\text{direction is } \sum_{i=1}^7 n_i = 2 \langle \Psi_0^u | \hat{S}_u | \Psi_0^u \rangle = g_i^S / 2$$

Table S2. Overlap integrals of the NSOs along direction 3. The total overlap interaction is $S_{AB} = 1.28 \cdot 10^{-8}$.

Overlap Integrals	NSO1B	NSO2B	NSO3B	NSO4B	NSO5B	NSO6B	NSO7B
NSO1A	1.25×10^{-4}	-5.25×10^{-5}	2.36×10^{-5}	-5.41×10^{-5}	-8.65×10^{-5}	-5.71×10^{-5}	4.75×10^{-5}
NSO2A	-5.25×10^{-5}	2.23×10^{-5}	-2.14×10^{-5}	1.40×10^{-5}	1.56×10^{-5}	-2.15×10^{-5}	-1.62×10^{-5}
NSO3A	2.36×10^{-5}	-2.14×10^{-5}	-5.58×10^{-7}	-1.84×10^{-5}	-2.05×10^{-5}	-1.72×10^{-5}	2.12×10^{-5}
NSO4A	-5.41×10^{-5}	1.40×10^{-5}	-1.84×10^{-5}	1.91×10^{-5}	2.12×10^{-5}	2.57×10^{-6}	-2.79×10^{-5}
NSO5A	-8.65×10^{-5}	1.56×10^{-5}	-2.05×10^{-5}	2.12×10^{-5}	4.24×10^{-5}	1.26×10^{-5}	-7.00×10^{-6}
NSO6A	-5.71×10^{-5}	-2.15×10^{-5}	-1.72×10^{-5}	2.57×10^{-6}	1.26×10^{-5}	-4.75×10^{-5}	-5.98×10^{-6}
NSO7A	4.75×10^{-5}	-1.62×10^{-5}	2.12×10^{-5}	-2.79×10^{-5}	-7.00×10^{-6}	-5.98×10^{-6}	6.64×10^{-5}
Occupation	0.599	0.557	0.461	0.38	0.222	0.141	0.007

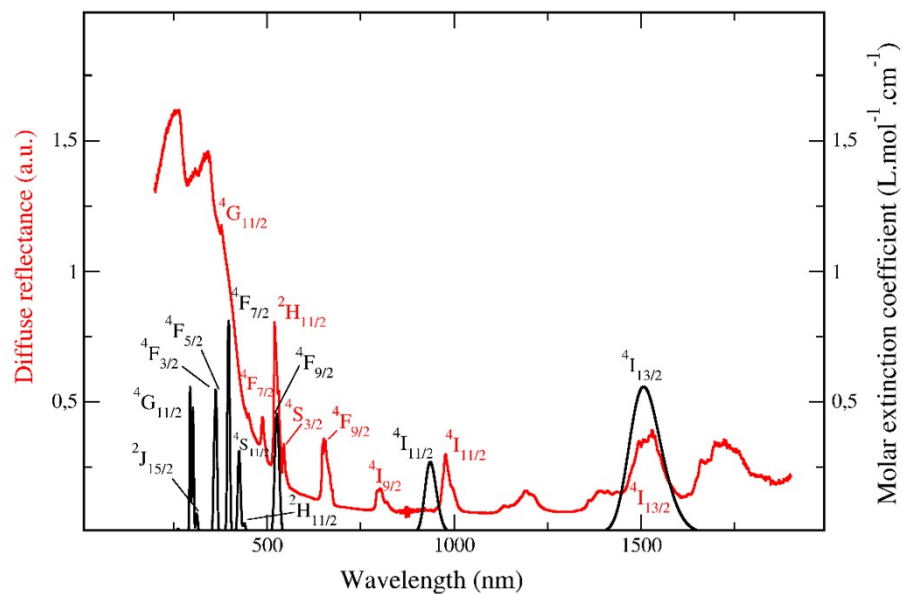


Figure S11. Calculated UV-visible spectrum at SO-CASSCF level (*black*) and experimental UV-Vis diffuse reflectance spectrum (*red*).